PHYSICAL REVIEW D VOLUME 44, NUMBER 11 1 DECEMBER 1991

Propagation of multi-TeV muons

Paolo Lipari
Istituto Nazionale di Fisica Nucleare, Sezione di Roma, and Department of Physics, University of Rome "La Sapienza" P'le Aldo Moro 2, Rome I-00185, Italy

Todor Stanev
Bartol Research Institute, University of Delaware, Newark, Delaware 19716
(Received 13 June 1991)

We discuss the propagation of muons of energy above a TeV through rock and stress the importance of correctly accounting for the fluctuations of the energy loss in radiative processes. Accounting for these fluctuations affects the major types of underground muon fluxes in the opposite way from a naive treatment that neglects the muon straggling. The rates of downward atmospheric muons are increased, while the flux of upward neutrino-induced muons is decreased. The paper analyzes the causes of these effects and gives helpful parametrizations for the muon ranges applicable to the two types of muon rates. We also extend our calculations to muon energies of 10^6 TeV and discuss the uncertainties in the muon energy loss at extremely high energy. An appendix gives a short review of the analytic techniques used to solve the problem of straggling and presents a toy model that displays the role of fluctuations in muon propagation. In another appendix we introduce an interesting technique for the generation of approximate energy, angular, and lateral distributions from the muon survival probability.

I. INTRODUCTION

The propagation of TeV muons through large depths of rock is an important tool in underground muon and neutrino physics. A good knowledge of the probability that a muon generated with energy E_0 will not be absorbed in X g/cm^2 of rock (survival probability $P_{\rm surv}$) is necessary to understand the most basic experimental result—the rate of single muons. The range distribution for muons arriving at the detector with energy E and the angular distribution of these muons is crucial for estimates of expected rates of upward-going, neutrino-induced muons of different origin. All these parameters plus the lateral displacement of the muons during propagation are needed for the analysis of the results on muon groups in terms of the chemical composition of the cosmic-ray flux.

The main energy-loss processes for TeV muons theoretically well understood. They are (i) ionization, (ii) bremsstrahlung, (iii) production of e^+e^- pairs, and (iv) photoproduction. While the ionization loss is only slowly logarithmically increasing with energy, the radiation processes cause a loss which in the high-energy limit is proportional to the muon energy. The average loss is usually expressed as

$$-\left\langle \frac{dE(E_\mu)}{dX} \right\rangle = \alpha + \beta E_\mu \ , \tag{1}$$

where α is due to ionization and β is the sum of the fractional radiation losses. If we assume that a muon of initial energy E_0, traversing each thin layer ΔX of a material, always loses the expected average: $\langle \Delta E(E_\mu) \rangle = \langle dE(E_\mu)/dX \rangle \Delta X$, we can calculate the "range of the average loss" as

$$R_{\langle \Delta E \rangle}(E_0) = \int_0^{E_0} \frac{dE_\mu}{\langle dE(E_\mu)/dX \rangle} = \frac{1}{\beta} \ln \left[1 + \frac{E_0}{\epsilon} \right] . \tag{2}$$

In the last equation we consider α and β energy independent, and define $\epsilon = \alpha/\beta$ as the muon critical energy at which the ionization loss equals the radiation loss. This is a good expression for the muon range when most of the energy loss is due to ionization and is thus continuous, i.e., for $E_\mu < \epsilon$. At higher energies the energy loss due to radiation starts to dominate. Fluctuations are inherent to the radiative processes and they replace $R_{\langle \Delta E \rangle}$ with a distribution of ranges. Some muons propagate much farther than $R_{\langle \Delta E \rangle}$ but the majority do not and the average range $\langle R \rangle$ becomes smaller than $R_{\langle \Delta E \rangle}$. This effect has been considered long ago in connection with the range of the electron.

The account for the fluctuations in the muon energy loss has two main consequences for the application to the underground muon and neutrino physics. First, muon propagation effects are energy dependent. The higher E_μ is, the bigger role fluctuations play. Correspondingly the R distribution becomes wider, and the $\langle R \rangle / R_{\langle \Delta E \rangle}$ ratio decreases. Second, the muon range distribution affects the estimates of the rate of down-going muons of atmospheric origin and the rate of upward-going neutrino-induced muons in the opposite way.

In the latter case the rate of upward-going muons explores the full muon range. It is thus sensitive to the average muon range, and accounting for the fluctuations will *decrease* the rate.

In the case of down-going muons one samples muons at a certain depth of rock X, and the steep cosmic-ray spectrum weights very heavily the fluctuations of the energy loss. The rate is $\int dE_\mu dN/dE_\mu P_{\rm surv}(E_\mu, X)$. A

small probability that relatively low-energy muons survive in the propagation is compensated by the much higher flux of such muons. The rate of muons is dominated by the small $P_{\rm surv}$ tail, and it is thus sensitive to the width of the range fluctuations, rather than to the average range. The accounting for the fluctuations should, correspondingly, *increase* the rate.

Analytic treatments of the fluctuations of the muon energy loss are only possible under the simplifying assumption that both α and β in Eq. (1) are energy independent. In fact α rises logarithmically with the energy. In the region up to 10 TeV, which is of utmost importance for deep-underground experiments, the high-energy limit (β=const) is not yet reached. Strictly speaking it is never reached as the energy loss to photoproduction increases logarithmically with energy. For this reason the analytic estimates of the muon range will always be inexact and approximate. A Monte Carlo propagation program, on the other hand, should be able to predict precisely not only the range, but all related parameters such as the muon energy distribution, angular and lateral spread at the observation level.

The analysis of experimental data from contemporary deep-underground experiments requires the use of Monte Carlo muon propagation codes, which are able to give good estimates of all these parameters. In this paper we discuss the features necessary for compiling of a good Monte Carlo program and describe our code in Sec. II. In Sec. III we present the basic results from runs of the code for standard rock and introduce some useful parametrizations. Section IV discusses the main applications of the results for underground muon physics. Section V contains an analysis of the uncertainties in the muon energy loss at extremely high energy. General conclusions are given in Sec. VI. We also present a compilation of analytic results on the muon propagation and a toy Monte Carlo model that demonstrates the importance of the fluctuations in Appendix A, and a fast algorithm for muon propagation in Appendix B.

Our Monte Carlo code, as well as a much faster code that samples from the results of the full Monte Carlo code to generate muon energy, angle, and lateral displacement after propagation on depth X, are available on request.

II. MUON INTERACTION CROSS SECTIONS AND MONTE CARLO ALGORITHMS

In a Monte Carlo treatment there is a significant difference between the ionization energy loss and the loss due to radiation. The fluctuations associated with the mechanism of ionization are relatively small. It is therefore a good approximation to treat this mechanism as "continuous," describing it by the mean value of the ionization loss per unit material thickness given by the well-known Bethe-Bloch formula [1] and accounting for the density effect.

The mechanisms (ii), (iii), and (iv) involve the radiation of a real or virtual photons. A complete description of these radiative processes is given by the differential cross sections $d\sigma_{\rm rad}(v,E)/dv$, where

$$v=\frac{E_\mu-E'_\mu}{E_\mu}=\frac{E_{\gamma(*)}}{E_\mu} \tag{3}$$

is the fraction of the muon energy transferred to the photon. The shape of $d\sigma_{\rm rad}(v,E)/dv$ determines the magnitude of the fluctuations in the muon propagation. The average energy loss for each radiative processes can be easily calculated as

$$\left\langle\frac{dE}{dX}\right\rangle_{\rm rad}(E)=\frac{N}{A}E_\mu\int_{v_{\min}}^{v_{\max}}dv\,v\left[\frac{d\sigma(v,E)}{dv}\right]_{\rm rad}. \tag{4}$$

N is the Avogadro number, A is the mass number of the material, and $v_{\min}$, $v_{\max}$ are the minimum and the maximum kinematically allowed fractional photon energies.

The cross section for pair production is always finite, while the cross section for bremsstrahlung and nuclear interactions diverge logarithmically when integrated over all possible values of v. This divergence corresponds to an infinite probability of radiating infinitely soft photons.

In the choice of cross sections we follow the compilation of Lohmann, Kopp, and Voss [2]. The original calculation of the differential cross section integrated over the directions of outgoing particles can be found in Ref. [3] for bremsstrahlung, Ref. [4] for pair production, Ref. [5] for photonuclear interactions. We will discuss the propagation of muons in "standard rock" ($A=22$, $Z=11$, $\rho=2.65$ g cm^{-3}). The formulas and parameters that fully define the ionization loss can be found in Ref. [6].

Asymptotically the differential cross sections for bremsstrahlung and pair production are energy independent and it is common to define

$$\beta_{\rm rad}(E)=-\frac{1}{E}\left\langle\frac{dE}{dX}\right\rangle_{\rm rad}=\frac{N}{A}\int_0^1 dv\,v\frac{d\sigma_{\rm rad}(v,E)}{dv}. \tag{5}$$

In Fig. 1 we show a graph of the quantities $\beta_{\rm brems}$,$\beta_{\rm pair}$,$\beta_{\rm nuc}$, and of their sum. An important point to consider is that the asymptotic values (full screening) of β for the purely electromagnetic processes is reached only at very high energy ($E_\mu\simeq 100$ TeV). For example, in standard rock at 0.1, 1, 10 TeV $\beta_{\rm brems}$ is 1.15, 1.47, and 1.63 [in units (10^{-6} g^{-1}cm^2)], $\beta_{\rm pair}$ is 1.56, 2.10, and 2.27, while the asymptotic values for the two processes are 1.70 and 2.32.

The contribution of the energy loss due to photonuclear interactions does not reach a constant value of β because of the expected growth of the photon-nucleon cross section $\sigma_{\gamma N}$ with energy: in the same units $\beta_{\rm nuc}=0.41$ at 1 TeV, and grows to 1.18 at 10^6 TeV. The photonuclear cross section is the most important element of this calculation that is not under complete theoretical control. We will discuss uncertainties related to this fact in Sec. V.

The general problem that we have to solve can be described as follows: we have a monoenergetic beam of muons of energy E_0 all moving along the z axis. We want to calculate the fraction of the flux that will reach the "detection" level $X(P_{\rm surv}(E_0,X))$, and the distribution of

kinematical properties of these muons after crossing depth X of a certain homogeneous medium of density ρ and well-defined composition. A detected muon can be fully defined by its energy E, angle θ, and lateral displacement l. In general we can define a distribution function $F(E,\theta,l;E_0,X)$ that describes fully the surviving muons. There are strong correlations among these variables, low final energies E correspond to large scattering angles and large lateral displacements.

The distribution function can be reduced to one dimension by integrations over the angular deviation and lateral displacement of the muon, obtaining the final energy spectrum $F(E,E_0,X)$. Integrating further over all energies we obtain the "survival probability" $P_{\rm surv}(E_0,X)$, or in general integrating from threshold energy $E_{\rm min}$ we can define a survival probability above a certain threshold $P_{\rm surv}(E_0,E_{\rm min},X)$.

In the literature there are several analytic solutions of the one-dimensional problem, and in Appendix A we briefly discuss these efforts. An analytic treatment is, however, possible only through approximations that are not completely adequate for high-precision studies. A full three-dimensional treatment is in practice only possible with Monte Carlo techniques.

An important, though trivial, requirement to a Monte Carlo procedure is that it has to implement all cross sections extremely precisely. Muon propagation to depths of 10^5–10^6 g/cm^2 takes thousands of samplings and a minor deviation from the true cross section easily adds up to large factors. Otherwise it is a straightforward problem. The complication connected to the divergent cross section can be avoided by the introduction of a "quasicontinuous" energy loss that represents very soft radiation. Therefore we can decompose the average energy loss into a "soft" part that is in the radiation of photons with energy below a certain threshold ($v<v_{\rm cut}$),

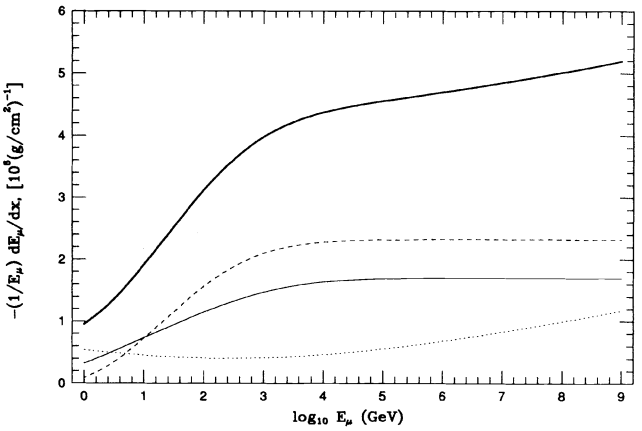

FIG. 1. Plot of the quantities $\beta_{\rm rad}=\langle dE/dx\rangle_{\rm rad}/E$ for the three radiative processes in standard rock as a function of the muon energy E. The solid line is for bremsstrahlung, dashed line for production of e^+e^- pairs, and the dotted line for photoproduction. The thick solid line shows the sum of the three processes.

that will be treated as a "continuous" loss and a "hard" part ($v\geq v_{\rm cut}$) that will be treated stochastically:

$$\left[\frac{dE}{dX}\right]_{\rm rad}=\left[\frac{dE}{dX}\right]_{\rm soft}+\left[\frac{dE}{dX}\right]_{\rm hard}$$
$$=\frac{N}{A}E\int_0^{v_{\rm cut}}dv\,v\frac{d\sigma(v,E)}{dv}$$
$$+\frac{N}{A}E\int_{v_{\rm cut}}^1 dv\,v\frac{d\sigma(v,E)}{dv}\ . \tag{6}$$

Note that the cross section for "hard radiation"

$$\sigma_{\rm hard}(E)=\int_{v_{\rm cut}}^1 dv\frac{d\sigma(v,E)}{dv} \tag{7}$$

is now always finite.

A muon of energy E crossing a thin layer of the medium of thickness dX will lose "continuously" due to soft radiation and ionization, $dE_{\rm soft}=\langle\alpha(E)+(dE/dX)_{\rm soft}\rangle dE$, and will have probability $dX/\lambda_{\rm hard}$ [with $\lambda_{\rm hard}=(\sigma_{\rm hard}N/A)^{-1}$] of radiating a photon of fractional energy $v\geq v_{\rm cut}$, the probability of radiating a quantum of energy v being proportional to the differential cross section $d\sigma/dv$.

An important question is what is a good value for $v_{\rm cut}$. Through trial and error we chose $v_{\rm cut}=0.01$ for the calculation. Smaller values increase the computing time, that is proportional to $\sigma_{\rm hard}\sim 1/v_{\rm cut}^2$. Larger values would begin to introduce a systematical bias in the estimate of the fluctuations.

The angular deviation of a muon is dominated by Coulomb multiple scattering, and for this reason we have neglected the angle of the muon acquired in the radiative processes using differential cross sections already integrated over all directions of the final particles. We have treated the multiple-scattering process in the Gaussian multiple-scattering approximation: a muon of initial energy E crossing a thin layer of material ΔX (g cm^{-2}) will emerge with a direction (θ_x,θ_y) and lateral displacement (l_x,l_y) distributed according to correlated Gaussians [7] (the initial direction of the muon is along the z axis, and the deviations in two orthogonal planes are independent):

$$\frac{d^2n}{d\theta_x\,dl_x}(l_x,\theta_x)=\frac{1}{\pi\sigma_l\sigma_\theta}$$
$$\times\exp\left[-\frac{2l_x^2}{\sigma_l^2}-\frac{2\theta_x^2}{\sigma_\theta^2}+\frac{2\sqrt{3}\theta_x l_x}{\sigma_l\sigma_x}\right] \tag{8}$$

the widths σ_θ and σ_l are given by the well-known expressions:

$$\sigma_\theta^2=\langle\theta_x^2\rangle=\langle\theta_y^2\rangle=\frac{\epsilon_{\rm ms}^2}{E^2}\frac{\Delta X}{\lambda_r}\ , \tag{9}$$

$$\sigma_l^2=\langle l_x^2\rangle=\langle l_y^2\rangle=\frac{1}{3}\frac{\epsilon_{\rm ms}^2}{E^2}\frac{\Delta X^3}{\rho^2\lambda_r}=\frac{1}{3}\left[\frac{\Delta X}{\rho}\right]^2\langle\theta_x^2\rangle\ , \tag{10}$$

where ρ is the density, λ_r is the radiation length, and

$\epsilon_{\rm ms} \simeq 0.014$ GeV (if the muon is not ultrarelativistic E has to be replaced with $p\beta$).

These expressions are valid if the layer is thin enough so that the energy of the particle can be considered as approximately constant, for a finite layer $\bar{X}$, we have to consider the energy loss. Equation (8) is still valid but σ_θ and σ_l are obtained from expressions

$$\sigma_\theta^2 = \frac{\epsilon_{\rm ms}^2}{\lambda_r} \int_0^{\bar{X}} dX \frac{1}{E(X)^2} , \tag{11}$$

$$\sigma_l^2 = \langle l_x^2 \rangle = \frac{\epsilon_{\rm ms}^2}{\rho^2 \lambda_r} \int_0^{\bar{X}} dX \frac{X^2}{E(X)^2} \tag{12}$$

(X is chosen so that $X=0$ is the point where the particle emerges from the scattering medium). In the case of the angular deviation the contribution of each layer $\Delta X \langle \Delta\theta \rangle = \sqrt{\Delta X}/E(X)$ is summed quadratically as in a standard random walk, each contribution is proportional to $E(X)^{-1}$. In the case of the lateral separations the contribution from layer X is weighted by a factor (X/ρ) the geometrical distance of the layer from the detection point.

The muons surviving at depth X will have a strongly non-Gaussian angular distribution with long tails. This qualitative result is true even if multiple scattering is treated in the Gaussian approximation because the fluctuations in the energy loss will induce large differences in the energy $E(X)$ of the muons at depth X. On average there is a nearly inverse proportionality between the energy of the emerging muon and its deviation angle, because most of the deviation is accumulated in the last part of the particle trajectory close to the detection level (see Appendix B for a more complete analysis of this point).

At very high muon energy the "continuous" energy loss and the angular and lateral displacements can be accounted for on one free path for "hard" loss. At energies comparable to ϵ the mean free path increases, while the multiple Coulomb scattering becomes more important, and the longitudinal step should be controlled so as not to distort the angular and lateral distribution. Since the angular deviation is inversely proportional to the muon momentum, a good way to do this is to use a step corresponding to a fixed fractional energy loss.

III. RESULTS FROM THE MONTE CARLO PROGRAM

It is impossible to present in a journal article enough results from the Monte Carlo propagation of high-energy muons to provide sufficient information for detector design or data analysis. For these reasons we only present here a limited number of results to demonstrate the effect of energy-loss fluctuations on the muon propagation and encourage the reader to use the Monte Carlo for all essential estimates.

A. Monoenergetic muon beam

Figure 2 shows the distributions of E_μ at depths, 1, 3, 5, 7, and 9 kilometers of water equivalent (1 km.w.e. $=10^5$ g/cm^2) for muons with $E_0 = 100$ TeV. The normalization of the histograms at different depths reflects the survival probability for these depths. At depth of 1 km.w.e. a significant fraction of the muons still carry a large fraction of E_0 as could be expected from the average energy loss. Certain number of muons, however, have already lost 2/3 of their energy. The distribution is wide and asymmetric with a very long tail toward low energy. At greater depths the distribution becomes even wider preserving the long low-energy tail.

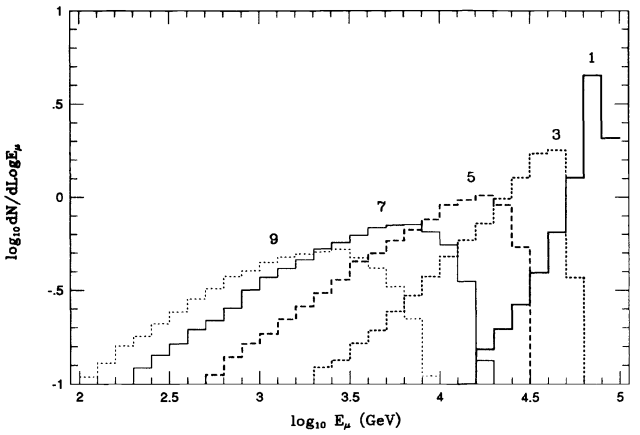

FIG. 2. Energy distribution of muons of $E_0 = 10^5$ GeV after propagation in standard rock to depths from 1 to 9 km.w.e. The numbers by the histograms show the corresponding depth.

In Fig. 3 we plot the survival probabilities $P_{\rm surv}(E_0, X)$ for E_0 from 1 to 10^6 TeV. The difference of the shape of $P_{\rm surv}$ is easily noticeable. The curves become flatter with increasing E_0, which reflects the increasing influence of the radiative energy loss and correspondingly the fluctuations in the energy loss. It is interesting to discuss these results in terms of the range of the average energy loss $R_{\langle \Delta E \rangle}$, which is indicated with an arrow by the corresponding survival probability curve.

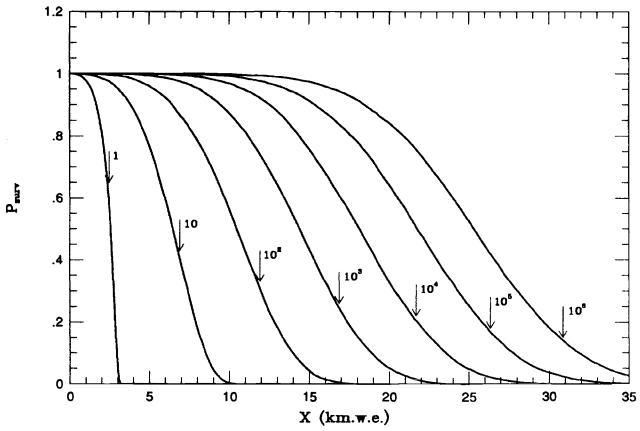

FIG. 3. Survival probabilities of muons of energy from 1 to 10^6 TeV in standard rock. E_0 is indicated by each curve. The arrows show the range of the average energy loss $R_{\langle \Delta E \rangle}$.

Although sometimes the range of the particle is longer than the "naive" definition (2) and sometimes shorter, a crucial point, important for the application of neutrino astronomy, is that the average range $\langle R \rangle$ is *smaller* than the naive definition. The effect of fluctuations is thus not only to broaden the range distribution, but also to shift the average value estimated from Eq. (2).

If we neglect fluctuations, then the three quantities (E_0, E_f, X), the initial and final energies of a muon crossing a depth X, are related by a well-defined condition

$$X = \int_E^{E_0} \frac{dE_\mu}{\langle dE(E_\mu)/dX \rangle} \tag{13}$$

and any of the three variables can be expressed as a function of the other two. Knowledge of the function $\langle dE(E_\mu)/dX \rangle$ is then sufficient to fully describe muon propagation (neglecting the "three-dimensional" effects of multiple scattering). For an explicit example, if the quantities β and α in Eq. (1) are independent of energy, and defining $\epsilon = \alpha/\beta$, the relation between the quantities (E_0, E, X) takes the very simple form

$$E = (E_0 + \epsilon)\exp(-\beta X) - \epsilon \ , \tag{14}$$

$$E_0 = (E + \epsilon)\exp(+\beta X) - \epsilon \ , \tag{15}$$

$$X = \frac{1}{\beta} \ln \left[\frac{E_0 + \epsilon}{E + \epsilon} \right] . \tag{16}$$

The simplicity of this approximation is tempting, unfortunately the effect of fluctuations is not negligible, and for any quantitative estimate must be taken into account.

B. Power spectrum muon beam

Figures 4–6 show the energy, angular and lateral distributions of muons surviving to depths of 3 and 10 km.w.e. These two depths bracket the depth range where we can expect reasonable statistics from the current deep-underground muon detectors. The primary muon beam has an $KE_0^{-3.7}$ differential energy spectrum, close to the one expected for muons generated by π and K decays in cosmic-ray cascades in the atmosphere. In the figures all distributions are shown normalized to unit area, the absolute normalization is discussed in Sec. IV A.

Let us first discuss the energy distributions. They are quite similar at the two depths, with the spectrum slightly harder at 10 km.w.e. $\langle E_\mu \rangle$ is 225 GeV at 3 km.w.e.

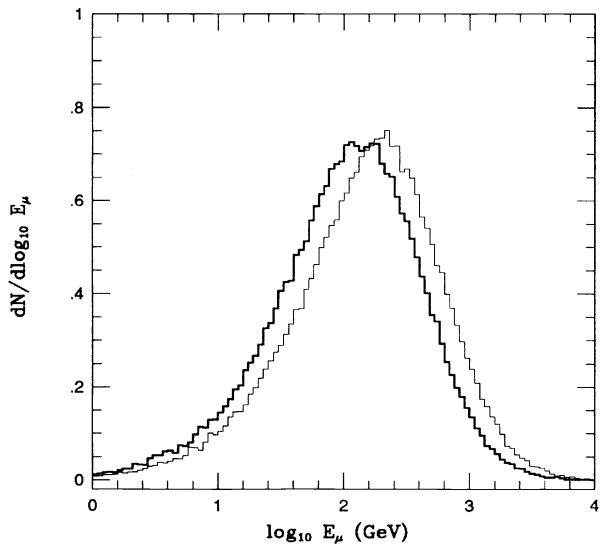

FIG. 4. Energy distribution of muons from a power spectrum with index $\gamma = 3.7$ at depths of 3 (thick line) and 10 (thin line) km.w.e.

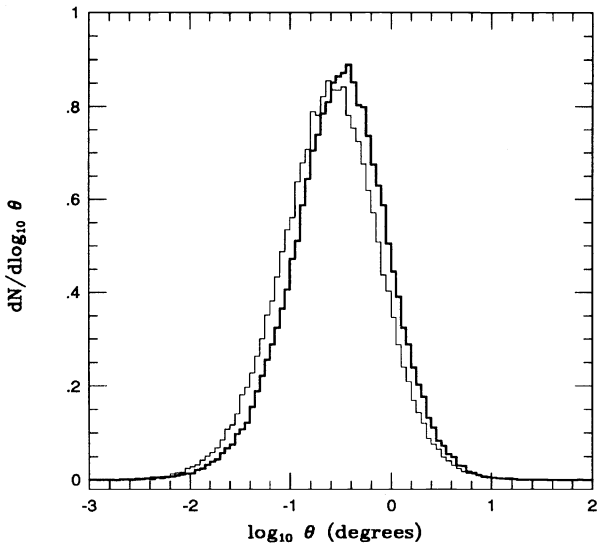

FIG. 5. Angular distribution of muons from a power spectrum with index $\gamma = 3.7$ at depths of 3 (thick line) and 10 (thin line) km.w.e.

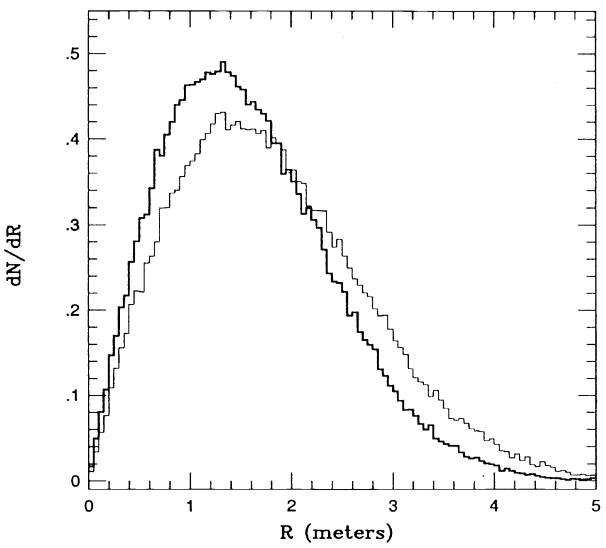

FIG. 6. Lateral distribution of muons from a power spectrum with index $\gamma = 3.7$ at depths of 3 (thick line) and 10 (thin line) km.w.e.

and 325 GeV at 10 km.w.e. Qualitatively the average values are similar to what one would expect in the case of no fluctuations. Using Eq. (13) and a power-law energy spectrum for the primary beam the muon energy spectrum at depth X will then be

$$\frac{dN}{dE_\mu}=Ke^{\beta x(1-\gamma)}[E_\mu+\epsilon(1-e^{-\beta X})]^{-\gamma}\ , \tag{17}$$

where γ is the spectral index of the primary beam. The spectrum will initially harden with the depth to reach a constant slope at very large depths. This picture is not only qualitatively true, but also quantitatively very close to the Monte Carlo output. It should be remembered, however, that the most important factor in Eq. (17) is the spectral index γ, which determines the overall shape of the local energy spectrum.

Figure 5 shows the local angular distribution of the muons at the two depths. The effect of the depth is now inverted, with a narrower distribution corresponding to the harder energy spectrum at 10 km.w.e. This effect is fully consistent with the general features of the multiple Coulomb scattering, which predict that the angular distribution will be determined during the last stages of the propagation. The lateral distribution of Fig. 6 is more complicated, since it reflects both the angular deflection and the total path length of the muons. We discuss in more detail the relations between the local energy, angular and lateral distributions in Appendix B.

IV. APPLICATIONS TO UNDERGROUND PHYSICS

A. Downward-going muons

In the case of downward-going muons we have an initial flux of muons $\phi_0(E_0)$ and we want to calculate the rate in an underground detector. In this discussion we are considering a fixed zenith angle, at large energies the atmospheric muon flux depends on the zenith angle θ approximately as $\propto(\cos\theta)^{-1}$, we are leaving this zenith-angle dependence implicit. Integrating over all scattering angles and energies we can calculate the depth-intensity relation. The underground intensity at depth X is

$$I(X)=\int dE_0\,\phi_\mu(E_0)P_{\rm surv}(E_0,X)\ . \tag{18}$$

In general, for a detector with an energy threshold $E_{\rm thr}$ we can calculate the intensity above a given threshold: $I(X,E_{\rm thr})$. It was shown in the previous section that the typical energy of the underground muons is of order of a few hundred GeV, and therefore if the threshold of the detector is of the order of a few GeV, or a fraction of a GeV, the intensity is not very sensitive to the exact value of $E_{\rm thr}$.

Many of the expected sources of high-energy muons will have an initial differential energy spectrum that is a power law $\phi_0(E_0)=KE_0^{-\gamma}$, and it is interesting to discuss the depth-intensity relation induced by these spectra. $\gamma=3.7$ is a good approximation of the shape of the bulk of atmospheric downward muons above 1 TeV; $\gamma=2.7$ corresponds to the expected energy distribution of muon produced by a prompt mechanism such as charm decay, $\gamma=2.0$ could be relevant in case of prompt muons production from an exotic primary from an astrophysical source.

A simple parametrization for $I(X)$ is suggested by the following considerations: if we assume that fluctuations in the energy loss are negligible (they are not), the survival probability is then a step function $P_{\rm surv}(E_0,X)=\theta[E_0-E_{\rm min}(X)]$, where $E_{\rm min}(X)$ is the muon energy corresponding to range X. If we make the further assumption that $E_{\rm min}(X)$ is well approximated by the form [8]: $E_{\rm min}=\epsilon(\exp(\beta X)-1)$ we can easily perform the integration in (18) obtaining the result

$$I(X)=K\frac{\epsilon^{-\gamma+1}}{\gamma-1}e^{-(\gamma-1)\beta X}(1-e^{-\beta X})^{-\gamma+1}\ . \tag{19}$$

This expression is a good parametric form for the depth-intensity relation because it automatically reproduces some of the important qualitative features of the exact result. At large depths we can approximate the expression $(1-e^{-\beta X})$ with 1, and we obtain a depth-intensity relation that falls exponentially with depth: $I(X)\propto e^{-X/X_0}$ with a slope $X_0\simeq[\beta(\gamma-1)]^{-1}$ related to the primary muon spectrum. The correction factor $(1-e^{-\beta X})^{-\gamma+1}$ is always larger than 1 and therefore $I(X)$ approaches the asymptotic exponential behavior from above. The relation $(X-\ln I)$ shows a curvature in the region below $\simeq 5$ km.w.e. with a positive second derivative. We will use the parametrization (19) to describe the results of a detailed numerical integral. We emphasize that the quantities β and ϵ have to be considered as simple parameters without a direct physical meaning.

In Fig. 7 we show the results of a calculation of the depth-intensity relation for power-law spectra $\phi_0(E_0)=(\gamma-1)E_0^{-\gamma}$ (E_0 is in TeV, the normalization is chosen to have an integral spectrum of value 1 at one TeV), with $\gamma=3.7$, 2.7, and 2.0. The points in the figure correspond to the integration (18) of the muon spectrum weighted by the survival probability, the curves are two

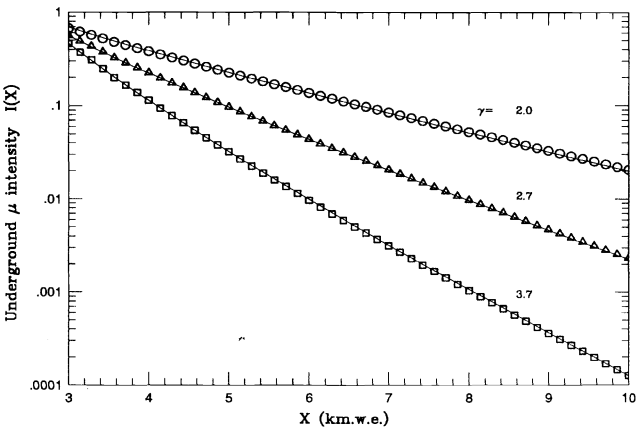

FIG. 7. Depth-intensity relations for muon spectra of different spectral index. The points are results of numerical integration over the E_0 spectrum and $P_{\rm surv}$. The lines show the fits described in Sec IV A.

parameter fits of form (19). The results of the fits are $\beta=0.383$ and $\epsilon=0.618$ for $\gamma=3.7$, $\beta=0.418$ and $\epsilon=0.557$ for $\gamma=2.7$, and $\beta=0.465$ and $\epsilon=0.569$ for $\gamma=2.0$. The fits have errors less than 4% for depths between 3 and 10 km.w.e. In comparison the fit of Gaisser and Stanev [8] overestimates the intensity by $\sim 20\%$ at shallow depths and crosses over our fit for $\gamma=3.7$ at 9 km.w.e.

Note that the fitted parameters β and ϵ depend on the exponent γ, that is on the shape of the incident spectrum. This may seem surprising if we naively think of the quantity $\epsilon(e^{\beta X}-1)$ as the threshold energy for a muon to penetrate to the depth X, which would lead us to conclude from the results of the fit, that muons with a steeper spectrum are somehow more penetrating than muons with flatter spectra. The qualitative behavior of the parameters can actually be easily understood. In the definition of the intensity (18) there is no sharp lower limit $E_{\min}(X)$, and the integrand, which is the product of two factors, one vanishing and the other rapidly growing, goes slowly to zero. The tails of P_{surv} are very important and muon energies that have survival probabilities of order 10^{-2}, 10^{-3} give still important contributions to the intensity because of the big enhancement due to their higher flux. Spectra of different shape give different weight to these tails, and this effect is absorbed in the fitted parameters β and ϵ. For a spectrum such as $E^{-3.7}$ where the flux falls by a factor of 5000 per decade the muon straggling results in an "effective threshold" significantly lower than for a flatter spectrum such as E^{-2}.

The importance of the tails also explains why the net effect of fluctuation is to significantly *enhance* the intensity over what one could calculate neglecting fluctuations. Note that the effective parameters β and ϵ are obtained by fitting a certain spectral shape and, if applied to estimates of intensity produced by a different source of muons (of different γ) would result in large errors.

B. Neutrino-induced muons

The muon yield $Y(E_\mu)$ of a neutrino of energy E_ν is defined as the average number of muons produced by the neutrino that will reach a detector, assuming that there is an infinite amount of material between the neutrino source and the detector and neglecting the absorption of the neutrinos. The detected muons will all be produced in the vicinity of the detector because even the highest-energy muons do not travel more than ~ 10 km, and therefore the assumption of "infinite amount of material" is essentially always well satisfied for directions below the horizon. The number of muons produced by a neutrino coming from nadir angle θ can be written in the factorized form

$$n_\mu = Y_\nu(E_\nu)\exp[-\sigma_{\text{tot}}(E_\nu)X(\theta)] , \tag{20}$$

where $X(\theta)$ is the column density of the Earth.

A muon detector will in general have an energy threshold for detection, and it is necessary to specify the yield of muons above this threshold as $Y(E_\nu\ ;E_{\min})$. In general we can write

$$Y_\nu(E_\nu;E_\mu^{\min}) = N_A \int_0^\infty dX \int_0^E dE_\mu \frac{d\sigma_\nu}{dE_\mu}(E_\mu;E_\nu) \times P_{\text{surv}}(E_\mu;E_\mu^{\min},X) , \tag{21}$$

where X is the distance (in g cm^{-2}) of the neutrino interaction point from the detector. The integral over the interaction point of the neutrino X can be performed first with the result

$$Y_\nu(E_\nu;E_\mu^{\min}) = N_A \int_0^{E_\nu} dE_\mu \frac{d\sigma_\nu}{dE_\mu}(E_\mu;E_\nu) R_{\text{eff}}(E_\mu,E_\mu^{\min}) , \tag{22}$$

where

$$R_{\text{eff}}(E_\mu;E_\mu^{\min}) = \int_0^\infty dX\, P_{\text{surv}}(E_\mu;E_\mu^{\min},X) \tag{23}$$

is a transparent equation because each produced muon is weighted by a production cross section and its range.

Note that if the survival probability has the form

$$P_{\text{surv}}(E_\mu;E_\mu^{\min},X) = \theta[R_{\langle\Delta E\rangle}(E_\mu,E_\mu^{\min}) - X] \tag{24}$$

then the yield can be rewritten as

$$Y_\nu(E_\nu;E_\mu^{\min}) = N_A \int_0^{E_\nu} dE_\mu \frac{d\sigma_\nu}{dE_\mu}(E_\mu;E_\nu) \times R_{\langle\Delta E\rangle}(E_\mu,E_\mu^{\min}) . \tag{25}$$

While Eq. (25) will overestimate the yield Y_ν because it uses the range of the average energy loss $R_{\langle\Delta E\rangle}(E_\mu,E_\mu^{\min})$, the use of R_{eff} in Eq. (22) accounts exactly for the fluctuations in the muon energy loss and is equivalent to taking the double integral of Eq. (21). Figure 8 shows R_{eff} as a function of E_μ for $E_\mu\min=1$, 10^2, 10^3, 10^4, 10^5, and 10^6 GeV. Apart from

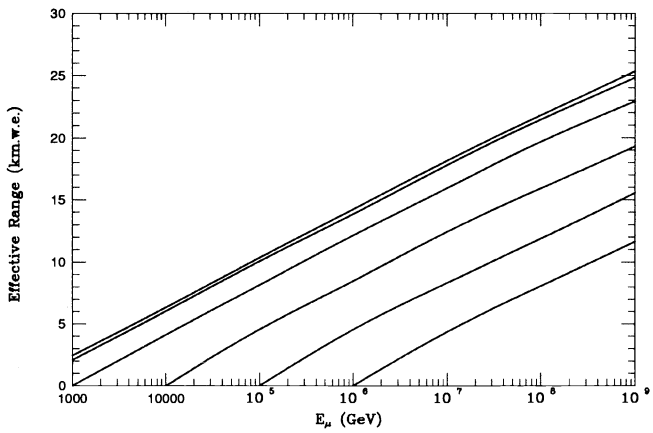

FIG. 8. Effective muon range as a function of E_0. Curves correspond to E_{thr} (from top to bottom) of 1, 10^2, 10^3, 10^4, 10^5, and 10^6 GeV.

the threshold effects at $E_\mu = E_\mu^{\min}$, $R_{\rm eff}$ is essentially linear with $\ln E_\mu$. The slight curvature at high E_μ values is due to the increase of the relative energy loss at very high energy. The different curves have approximately the same slope. For large values of the threshold energy $E_\mu^{\min}$ the curves are also nearly equispaced, this reflects the fact that when radiative processes are dominant a muon of energy E will on average lose a fixed fraction of its energy in a depth X approximately independent of E. When $E_\mu^{\min}$ is sufficiently small, ionization losses become important and the distance between the curves decreases (note that there is no curve for $E_\mu^{\min} = 10$ GeV).

V. UNCERTAINTIES IN THE MUON ENERGY LOSS

Although not experimentally studied at TeV energies the muon energy loss is theoretically very well understood. Our calculations are thus very reliable when the muon beams to be propagated have a steep energy spectrum and the major contribution is from few to few tens of TeV. This is the case of muons generated in cosmic-ray atmospheric cascades. There are, however, predictions of astrophysical [9] or cosmological [10] neutrino fluxes that extend to energies of 10^6 TeV and are detectable mostly through the muons (approximately with the same energy) that they generate in deep-inelastic scattering. At such extreme energies there are two effects that could alter the energy-loss formulas used in this paper.

At very high energy and materials as dense as standard rock the Landau-Pomeranchuk-Migdal [11] (LPM) effect becomes gradually important for the muon radiation processes. The effect is due to interference between the atomic fields of single atoms when the interaction region becomes comparable to the radiated photon wavelength and results in a suppression of the radiation cross sections. It affects first the radiation of soft photons, and is therefore most important for the bremsstrahlung energy loss. We did a calculation of the bremsstrahlung energy loss of muons in standard rock using the formulas of Migdal [11]. The effect becomes noticeable at 10^4 TeV and leads to a 10% decrease of $\beta_{\rm brems}$ at 10^6 TeV. Considering the extreme muon energy, the moderate effect, and the theoretical uncertainties we decided not to account for the LPM effect in the current calculation. An account for the effect would have of course slightly increased the muon range at 10^6 TeV.

A potentially more dangerous effect might arise from the photoproduction cross section. The real photon cross section on nucleons $\sigma_{\gamma N}$ is an explicit part of the muon photoproduction cross section. If $\sigma_{\gamma N}$ has a strongly energy-dependent QCD component, due to a certain gluonic content of the photon [12], then the muon photoproduction energy loss will be strongly affected and might become the major energy-loss process. Figure 9 shows the average energy loss to photoproduction in three assumptions for the energy behavior of $\sigma_{\gamma N}$. The solid line is the cross section [5] used in this calculation which has a small $\ln^2(s)$ term. The dotted line is a low-energy fit with a $\ln(s)$ term, while the dashed line uses an eikonalized QCD cross section [13] with the photon structure functions of Drees and Grassie [14]. It is similar to the photoproduction cross sections calculated with the same structure functions by Gandhi *et al.*[15], who also predict a much faster growth with a different set of structure functions. Such photoproduction cross sections would turn muon photoproduction into the most important energy-loss process. It would also affect the energy loss at moderate energies ~ 10 TeV. Most recent considerations [16], however, seem to rule out such fast growth of $\sigma_{\gamma N}$.

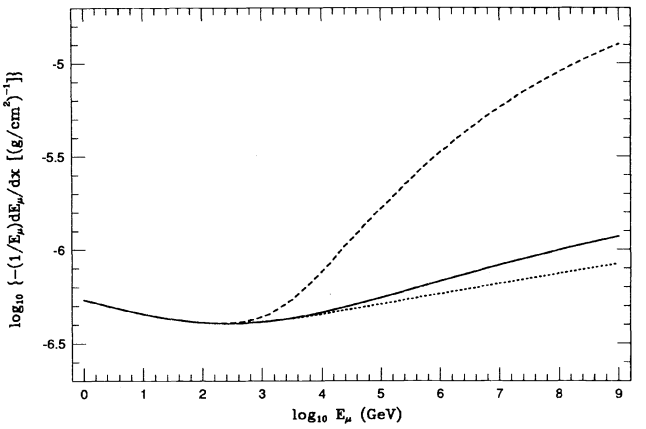

FIG. 9. $\beta_{\rm phot}$ in different assumptions for $\sigma_{\gamma N}$. See text for the codes of the different curves.

VI. CONCLUSIONS

We have shown that accounting for the fluctuations in the muon energy loss is essential for the estimates of the muon range and for the calculations of the muon rates in deep-underground muon detectors. The effects of muon straggling on the rates of atmospheric and neutrino-induced muons are in opposite directions. The calculation of the rate of neutrino-induced upward-going muons is sensitive to the entire distribution of muon ranges, whose average is decreased by the fluctuations in the energy loss. The estimate of the rate of atmospheric muons, on the other hand, involves the tail of the survival probability, and is thus increased in comparison with estimates neglecting the straggling.

We have performed Monte Carlo calculations of the propagation of multi-TeV muons through large thickness of standard rock and have fitted the results to simple useful parametrizations. The analysis of muon data, however, requires a full Monte Carlo treatment, which can generate the correlations between the local muon energy, angular and lateral distributions and account for the rock composition at the detector site, which can cause the biggest uncertainty in the propagation of TeV muons. The Monte Carlo code for muon propagation is available on request.

At extremely high muon energies, relevant for the detection of diffuse fluxes of ultra high-energy neutrinos, one should be aware of the uncertainties in the muon radiation cross sections caused by the LPM effect and the photon interaction cross section.

ACKNOWLEDGMENTS

We are grateful to Dr. T. K. Gaisser for his encouragement to put these results on paper. P. L. thanks Professor P. Pistilli for initially suggesting muon propagation as an important research topic. This work was supported in part by the National Research Foundation. P. L. appreciates the hospitality of the Bartol Research Institute during the time this paper was written.

APPENDIX A: ANALYTIC SOLUTIONS AND A TOY MODEL

Several authors have discussed how to calculate with analytic methods the differential or integral spectrum of the muons of initial energy E_0 that reach depth X. These efforts have a long history. Already in 1934 in their original work on electron bremsstrahlung, Bethe and Heitler [17] suggested an analytic solution for the spectrum of electrons after propagation to depth X neglecting the "regeneration" of electrons due to pair production. Their elegant solution (A8) is not a bad approximation for very-high-energy muons. The mathematical techniques used to tackle this problem are identical to those used in the study of electromagnetic shower theory [18]. In fact this problem is formally identical to a very simplified version of shower theory where photons do not produce e^+e^- pairs.

The function $F(E,E_0,t)dE$, that describes the probability of finding a particle at a depth t with energy between E and $E+dE$ after the propagation of a muon of initial energy E_0 satisfies the integrodifferential equation

$$\frac{\partial F(E,t)}{\partial t}=-\int dv\left[F(E,t)\varphi(v,E)-\frac{1}{1-v}F\left[\frac{E}{1-v},t\right]\varphi\left[v,\frac{E}{1-v}\right]\right]+\frac{\partial[\alpha(E)F(E,t)]}{\partial E} \tag{A1}$$

with the boundary condition $F(E,0)=\delta(E-E_0)$. In this equation $\alpha(E)$ is the energy loss for ionization and $\varphi(v,E)$ is the differential cross section (summing over all radiation processes) for radiating a fraction v of the energy:

$$\varphi(v,E)=\frac{N_A}{A}\sum_{\text{rad}}\frac{d\sigma_{\text{rad}}}{dv}(v,E)\ . \tag{A2}$$

Solutions to Eq. (A1) can be found using two approximations, that are equivalent to approximations A and B of shower theory. Approximation A consists of two assumptions:

(i) $\varphi(v,E)$ is considered independent of E.

(ii) The ionization loss is neglected.

In approximation B, the second assumption is replaced by the following.

(ii') The ionization loss α is a constant.

In both cases it is possible to unambiguously define an energy-independent radiation length,

$$\frac{1}{X_0}=\frac{N}{A}\int_0^1 dv\, v\frac{d\sigma(v)}{dv}\ , \tag{A3}$$

and we can measure depth in units of radiation lengths $t=X/X_0$.

The propagation problem in approximation A can be easily solved, at least formally. The Mellin transform of the differential and integral spectra F and $G[P_{\text{surv}}(E_0,t)=G(0,E_0,t)]$ have the simple expressions

$$M_F(s;E_0,t)=\int_0^\infty dE\, E^s F(E,E_0,t)=E_0^s\exp[tA(s)]\ , \tag{A4}$$

$$M_G(s;E_0,t)\int_0^\infty dE\, E^s G(E,E_0,t)=\frac{E_0^{s+1}}{s+1}\exp[tA(s+1)], \tag{A5}$$

where

$$A(s)=\int_0^1 dv[1-(1-v)^s]\varphi(v)\ . \tag{A6}$$

The inversion of the Mellin transform requires an integral in the complex field:

$$f(x)=\frac{1}{2\pi i}\int_{\delta-i\infty}^{\delta+i\infty} ds\, x^{-(s+1)}M_f(s) \tag{A7}$$

and in general cannot be performed analytically. The standard technique is to evaluate the integral (A7) with the saddle-point approximation method [18].

In their original work [17] Bethe and Heitler approximated the shape of $\varphi(v)$ with the form $\varphi(v)=-[\ln 2\ln(1-v)]^{-1}$, then $A(s)=\ln(1+s)/\ln 2$, and the final result can be calculated exactly as

$$F(E,E_0,t)=\frac{1}{E_0}\frac{[\ln(E_0/E)]^{(t/\ln 2-1)}}{\Gamma(t/\ln 2)}\ . \tag{A8}$$

The solution of Eq. (A1) in approximation B is significantly more complicated. As in approximation A the steps are to first calculate the Mellin transform of the energy spectrum and then to use a saddle-point approximation method to invert it. The functions M_F and M_G can be written as power series. Two different expansions are useful. One possible expression [19,20] for M_F and M_G is appropriate for depths that are small compared to X_0, and involves an expansion in powers of t. A different expression [20] is appropriate for depths large compared to X_0 and involves an expansion in power of ϵ/E where $\epsilon=\alpha X_0$. We refer the reader to the original literature for the explicit formulas and a more complete discussion.

Some remarks are due.

(1) The saddle-point approximation method introduces small numerical errors in the final results, especially when t is small, a numerical inversion of the Mellin transform requires a knowledge of $A(s)$ in the complex field and complicates significantly the evaluation of the spectra.

(2) The approximations (i) and (ii') are not fully justified in the region (E_0,X) that is important for underground studies and introduce small but significant biases in the calculation.

A toy model

As an example that is easier to visualize we want to briefly discuss a toy model of the propagation of a hypothetical particle that loses a constant amount of energy to "ionization" and suffers "radiation" loss that is described by an exactly scaling differential cross section $d\sigma(v)/dv$. Choosing the units in an appropriate way: depth measured in radiation length and energy in units of the critical energy $\epsilon=\alpha X_0$ the average energy loss can be written as

$$\left\langle \frac{dE}{dX} \right\rangle = 1+E \ . \tag{A9}$$

Neglecting fluctuations the range of the average loss is $R_{\langle \Delta E \rangle}=\ln(1+E)$. To study the effect of fluctuations we will consider the artificial form

$$\varphi(v)=(n+1)(n+2)(1-v)^n \ , \tag{A10}$$

where n is a free parameter. The cross section for radiation in units (radiation lengths)$^{-1}$ is $\sigma_{\rm rad}=(n+2)$, and the average fractional energy of a radiated quantum is $\langle v \rangle = 1/(n+2)$. The average energy loss for radiation $\langle dE/dx \rangle_{\rm rad}=E\langle v \rangle \sigma_{\rm rad} N/A$ is independent from the exponent n, but increasing n corresponds to more frequent radiation of softer quanta. The limit $(n \to \infty)$ corresponds to a differential cross section $\varphi(v) \to \delta[v]/v$, or to the infinitely frequent emission of quanta of vanishing energy, i.e., to continuous energy loss with no fluctuations.

The survival probability in this model can be easily calculated by Monte Carlo or analytic techniques. This allows us to study how the result is affected by fluctuations in the energy loss, that critically depend on the shape of the differential cross section.

In Fig. 10 we show the survival probability $P_{\rm surv}(E,X)$ for a particle with 100 times the critical energy, and four values of exponent ($n=0,2,10$, and 100). We can verify three important qualitative effects.

(1) The effect of fluctuations is stronger for a harder radiation spectrum, or correspondingly for smaller values of n.

(2) The effect is not only to broaden the distribution but to shift the average range of the particles.

(3) There is a tail of particles that have ranges longer than the naive expectation $R_{\langle \Delta E \rangle}=\ln(1+E)$ and this tail is more pronounced for harder radiation spectra.

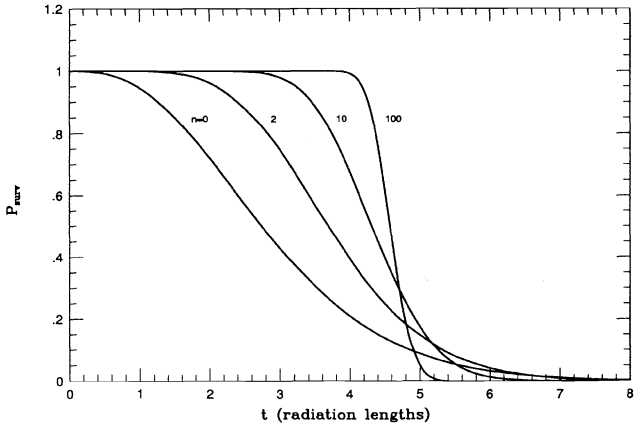

FIG. 10. Survival probabilities in the toy model described in Appendix A.

APPENDIX B: AN APPROXIMATE ALGORITHM FOR MUON PROPAGATION

We have made conscious efforts to develop a Monte Carlo code that runs reasonably fast, but the amount of computations necessary for the simulation of the muon signal in underground detectors remains large. It is easy to calculate with great precision the survival probability $P_{\rm surv}(E_0,X)$ in given material and interpolate from a tabulation in muon energy and material thickness, it is however much more complicated to parametrize in a detailed and precise way the function $F(E,\theta,l;E_0,X)$ that describes the distribution of energy E, angular deviation θ and lateral displacement l of those μ's of initial energy E_0 that survive at depth X. For many physical applications a precise knowledge of this distribution function is of great importance, and the only practical solution is a direct Monte Carlo calculation of the desired distributions. This calculation is very expensive especially because (as a consequence of the steepness of the cosmic-ray spectrum) a large fraction of the underground muon signal is produced by muons with small $P_{\rm surv}$, and each sampling of the distribution function F requires the propagation of many particles. The idea of devising "shortcuts" to the full Monte Carlo propagation that are sufficiently precise is therefore very appealing.

In this appendix we discuss algorithms that allow us to calculate with good approximation and in a negligible computer time the distribution function $F(E,\theta,l;E_0,X)$, assuming a precise knowledge of the survival probability $P_{\rm surv}(E_0,X)$. The fundamental ideas behind these algorithms are two: (i) the shape of the survival probability contains in integral form information about the muon energy spectrum at all depths; (ii) the energy distribution at a given depth allows the reconstruction of the three-dimensional distribution of the muon signal.

1. Energy distribution

Let us consider the muons with initial energy E_0 propagated to depth X_0. At this depth there will be a number $F(E_f;E_0,X_0)dE_f$ of muons with energy between E_f and E_f+dE_f. If we can neglect the fluctuations in the energy loss (this in general is not true, but it is approximately correct for muons below a few hundred GeV), and $R(E)$ is the range of a particle of energy E, then these muons will range out after traveling an additional thickness between $R(E_f)$ and $R(E_f+dE_f)$; therefore,

$$F(E_f;E_0,X_0)dE_f = P_{\text{surv}}[E_0,X_0+R(E_f)]-P_{\text{surv}}[E_0,X_0+R(E_f+dE_f)]$$
$$= -\left[\frac{dP_{\text{surv}}}{dX}(X,E_0)\right]_{X=X_0+R(E_f)}\left[\frac{dR(E)}{dE}\right]_{E=E_f}dE_f \ . \tag{B1}$$

Using the approximate but explicit expression of the energy-range relation [Eq. (16)] we obtain the result

$$F(E_f;E_0,X_0) = -\left[\frac{dp_{\text{surv}}}{dX}(E_0,X)\right]_{X=X_0+1/\beta\ln(1+E_f/\epsilon)}\frac{1}{\beta}\left[\frac{1}{E_f+\epsilon}\right] . \tag{B2}$$

In other words, the shape of the survival probability curve for $X \geq X_0$ can be used to describe the energy distribution of the muons surviving to depth X_0. If we know $P_{\text{surv}}(E_0,X)$ for all values of $X \geq X_0$ we can generate the energy spectrum at X_0 according to Eq. (B2) with the following steps.

(1) Compute $p_0 = P_{\text{surv}}(E_0,X_0)$.

(2) Generate a probability p flatly distributed between limits: $0 \leq p \leq p_0$.

(3) Solve the implicit equation: $P_{\text{surv}}(E_0,X)=p$ for X.

(4) The quantity $E_f = \epsilon(e^{\beta(X-X_0)}-1)$ is now distributed according to Eq. (B2).

The algorithm we have described is correct only if the spectrum $F(E;E_0,X)$ vanishes for E larger than a few hundred GeV, because then for the muons that are present at depth X (and have already underwent large fluctuations in the energy loss) radiative processes are relatively unimportant, and the approximation of neglecting fluctuations in the remaining part of the trajectory is adequate. The fraction of cosmic-ray muons above 1 TeV in deep-underground experiments is of the order of 5% and therefore this approximation is good in many practical circumstances. The results obtained with the algorithm described above for the propagation of muons with a power-law spectrum are in good agreement with the results obtained with a complete Monte Carlo procedure.

The algorithm just described deforms the true energy spectrum if a significant fraction of the muons present at the depth X_0 are above 1 TeV. This is the case for very high energy or for a very small depth. To understand the failure of the algorithm it is instructive to apply it to the extreme case of $X_0=0$. In this case the true energy distribution is a delta function $\delta(E-E_0)$, while the algorithm described above gives a finite width distribution.

2. Angular deviation and lateral displacement

The solution of the unidimensional propagation problem allows us also to solve (always in an approximate way) the three-dimensional propagation problem. If we continue to neglect the fluctuations, we can assume that a particle that reaches the detection level X_0 with energy E_f had energy $E(t)=[(E_f+\epsilon)e^{\beta t}-\epsilon]$ at depth (X_0-t). If we treat multiple scattering in the Gaussian approximation in each layer, and the energy loss is continuous, then the final deviation of a particle is still distributed as a Gaussian. Inserting this explicit form of $E(t)$ in Eq. (11) we obtain the result

$$\sigma_\theta^2(E,X_0) = \frac{\epsilon_{\text{ms}}^2}{\lambda_{\text{rad}}}\int_0^{X_0}dt\frac{1}{E(t)^2}$$
$$= \left[\left(\frac{\epsilon_{\text{ms}}}{\epsilon}\right)^2\frac{1}{\beta\lambda_{\text{rad}}}\right]f_\theta(E,X_0) \tag{B3}$$

with

$$f_\theta(E_0,X_0) = -\frac{E_0+\epsilon}{E_0}+\frac{E_0+\epsilon}{E_0+\epsilon(1-e^{\beta X_0})}$$
$$+\ln\left[1+\frac{\epsilon}{E_0}(1-e^{\beta X_0})\right] . \tag{B4}$$

It is interesting to note that the limit

$$\lim_{X_0\to\infty} f_\theta(E_f,X_0) = \frac{\epsilon}{E_f}+\ln\left[\frac{E_f}{E_f+\epsilon}\right] \tag{B5}$$

is well defined and finite, and that actually it is reached rapidly. The physical significance of this fact is that the multiple scattering of a muon is accumulated in the last part of the trajectory because the multiple-scattering angle in each layer is inversely proportional to $E(t)$. For sufficiently large X_0 one can neglect the initial part of the trajectory. The overall angular distribution will be the superposition of many Gaussians, each corresponding to a certain final energy, and will be strongly non-Gaussian.

The approximation we are discussing is good if most of the muons at the detection level X_0 have energies low enough so that the radiation processes are not very important. The multiple-scattering angle is accumulated not too far from the detection level, and the large fluctuations in the energy loss have already played their role producing a broad energy spectrum, and are therefore correctly taken into account by the use of the true energy distribution at the detection level.

It is worth stressing that the angular distribution is really dominated by the large fluctuations in the radiative energy losses. The tails of the angular distributions are populated not so much by particles that underwent unlikely very-large-angle scatterings, but mainly those particles that are close to ranging out. The essential ingredient in a calculation of a correct angular distribution is a precise calculation of the low-energy part of the muon energy distribution at the detector level. This consideration helps to understand why in a full Monte Carlo code the use of more sophisticated treatments of the angular deviations in a thin layer of material (Moliere scattering instead of Gaussian scattering) has a very small

effect on the final distributions.

A similar argument can be developed for the lateral displacement. The lateral distribution of particles with final energy E_f can be well approximated by a Gaussian of width that depends essentially only of E_f. Inserting the expression $E(t)=(\epsilon+E_f)e^{\beta t}-\epsilon$ in Eq. (12) we can calculate the width σ_l:

$$\sigma_l^2(E_f,X_0)=\frac{\epsilon_{\rm ms}^2}{\rho^2\lambda_r}\int_0^{X_0}dt\frac{t^2}{E(t)^2}$$
$$=\left[\frac{\epsilon_{\rm ms}^2}{\epsilon^2\beta^3\rho^2\lambda_r}\right]\int_0^{\beta X_0}dz\frac{z^2}{[(1+E_f/\epsilon)e^z-1]^2}\ . \tag{B6}$$

The final integration cannot be performed analytically but can be easily calculated numerically, and it also converges [somewhat sower than Eq. (B3)] for $X_0\rightarrow\infty$.

For completeness we note that if we use for $E(t)$ the simple expression $E(t)=E_f+\alpha t$ that is approximately valid for low energy we have

$$\sigma_l^2(E_f,X)=\frac{\epsilon_{\rm ms}^2}{\rho^3\lambda_r}\frac{X}{\alpha^2}\left[1+\frac{1}{1+y}-\frac{2}{y}\ln(1+y)\right]\ , \tag{B7}$$

where $y=\alpha X/E_f$. It is easy to check that the expression in large parentheses goes to zero when $y\rightarrow 0$ as $y^2/3$, and then the expression has the correct form for $X\rightarrow 0$.

We have a code PROPFAST that uses survival probability tables in standard rock to return the quantities $(E_f,\theta_x,\theta_y,l_x,l_y)$, that kinematically completely describe a muon of primary energy E_0 after propagation at depth X, using the algorithms described in this appendix.

[1] R. M. Sternheimer and R. F. Peierls, Phys. Rev. B **3**, 3681 (1971).

[2] W. Lohmann, R. Kopp, and R. Voss, CERN Yellow Report No. EP/85-03.

[3] A. A. Petrukhin and V. V. Shestakov, Can. J. Phys. **46**, S377 (1968).

[4] R. P. Kokoulin and A. A. Petrukhin, in *Proceedings of the XII International Conference on Cosmic Rays* (Hobart, Tasmania, Australia, 1971), Vol. 6.

[5] L. B. Bezrukov and E. V. Bugaev, Yad. Fiz. **33**, 1195 (1981) [Sov. J. Nucl. Phys. **33**, 635 (1981)].

[6] R. M. Sternheimer *et al.*, At. Data Nucl. Data Tables **30**, 261 (1984).

[7] B. Rossi, *High Energy Particles* (Prentice Hall, Englewood Cliffs, NJ, 1952).

[8] T. K. Gaisser and T. Stanev, Nucl. Instrum. Methods **A235**, 183 (1985).

[9] F. W. Stecker, C. Done, M. H. Salamon, and P. Sommers, Phys. Rev. Lett. **66**, 2697 (1991).

[10] C. T. Hill and D. N. Schramm, Phys. Rev. D **31**, 564 (1985).

[11] A. B. Migdal, Phys. Rev. **103**, 1811 (1956).

[12] M. Drees and F. Halzen, Phys. Rev. Lett. **61**, 275 (1989).

[13] T. K. Gaisser, F. Halzen, T. Stanev, and E. Zas, Phys. Lett. B **243**, 444 (1990).

[14] M. Drees and K. Grassie, Z. Phys. C **28**, 451 (1985).

[15] R. Gandhi, I. Sarcevic, A. Burrows, L. Durand, and H. Pi, Phys. Rev. D **42**, 263 (1990).

[16] R. Fletcher, T. K. Gaisser, and F. Halzen, Phys. Rev. D (to be published).

[17] H. Bethe and W. Heitler, Proc. R. Soc. **A146**, 83 (1934).

[18] B. Rossi and K. Greisen, Rev. Mod. Phys. **13**, 240 (1941).

[19] L. Eyges, Phys. Rev. **76**, 264 (1949).

[20] S. Hayakawa, J. Nishimura, and Y. Yamamoto, Prog. Theor. Phys. Suppl. **32**, 104 (1964).